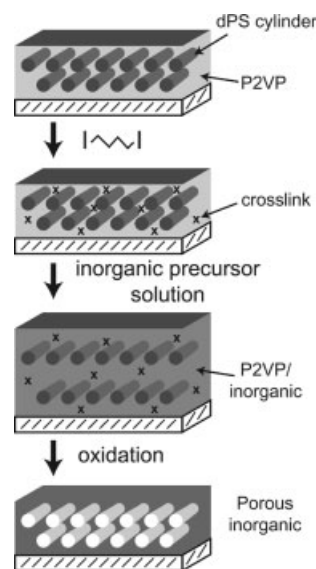


## Crosslinked Poly(styrene)-*block*-Poly(2-vinylpyridine) Thin Films as Swellable Templates for Mesostructured Silica and Titania\*\*

By Ryan C. Hayward, Bradley F. Chmelka, and Edward J. Kramer\*

Traditional approaches to the formation of mesostructured inorganic films from block-copolymer and surfactant templates rely on simultaneous assembly of amphiphilic structure-directing agents and inorganic sol-gel precursor species into ordered hybrid structures.<sup>[1-4]</sup> Variations in sample composition and processing conditions have afforded considerable control over the local (nanometer-scale) morphology of the composite mesostructures formed via such routes.<sup>[5]</sup> However, the ability to manipulate mesophase orientation and long-range ordering in these systems has been relatively limited so far,<sup>[6-12]</sup> largely due to restrictions on the timescale and conditions for processing that are imposed by network formation of the inorganic component. Here, we demonstrate an alternative approach to forming mesostructured inorganic thin films that can potentially circumvent these limitations. Pre-organized block-copolymer films are first crosslinked, allowing their morphology to be preserved as they are subsequently infiltrated with sol-gel species to form hybrid inorganic/organic materials. Specifically, thin films of poly(*d*<sub>8</sub>-styrene)-*block*-poly(2-vinylpyridine) (dPS-*b*-P2VP) diblock copolymer were thermally annealed to produce a well-ordered mesostructure consisting of dPS cylinders surrounded by a P2VP matrix. The cylinders were oriented parallel to the film plane due to preferential wetting of dPS at the free interface and P2VP at the substrate. As shown schematically in Figure 1, this morphology was fixed by chemical crosslinking of the majority P2VP component, allowing films to be swelled by aqueous solutions with essentially affine deformation of the polymer mesostructure. Sol-gel precursors for silica or titania present in the



**Figure 1.** Schematic illustration of the process employed for producing mesostructured and mesoporous inorganic replicas of crosslinked block-copolymer thin films.

swelling solution were sequestered into the P2VP component of the polymer, producing composite inorganic/organic replicas of the initial block-copolymer morphology. Subsequent oxidation to remove the block-copolymer template species led to mesoporous inorganic oxide films that closely resembled the original block-copolymer mesostructure. This decoupling of self-assembly from inorganic infiltration provides the possibility of first processing the block-copolymer film to obtain the desired mesostructural ordering, domain alignment, and surface patterning (using a variety of recently reviewed methods<sup>[13]</sup>) and subsequently forming a mesostructured inorganic replica of the starting template film.

Recently, other approaches have been described for the preparation of mesoporous silica from pre-formed films of organic templates. Sol-gel precursors were infused via supercritical CO<sub>2</sub><sup>[14]</sup> or via the vapor phase<sup>[15,16]</sup> into pre-formed films of non-crosslinked structure-directing agents, where they were subsequently condensed to produce ordered silica/organic hybrid materials. These approaches, and the current technique, can be thought of as an extension to thin films of the “true liquid-crystal templating”<sup>[17]</sup> approach for the formation of bulk mesoporous silica, wherein a pre-formed lyotropic liquid-crystal phase can be used as a template. However, as Nishiyama and co-workers<sup>[15,16]</sup> demonstrated, the use of a non-crosslinked organic structure-directing agent allows mesostructural rearrangement to occur until halted by the formation of a percolating silica network, potentially resulting in re-organization or even disorganization of the initial structure. In this key respect, these preparation techniques are similar to previous methods for the production of mesoporous silica films.<sup>[1-4]</sup> The ultimate structure depends on a cooperative assembly of the structure-directing agent and the inorganic component, and is therefore not a direct replica of the pre-existing template film.

[\*] Prof. E. J. Kramer, Dr. R. C. Hayward, Prof. B. F. Chmelka  
Department of Chemical Engineering, Department of Materials  
University of California, Santa Barbara, CA 93106 (USA)  
E-mail: edkramer@mrl.ucsb.edu

[\*\*] We thank Dr. Azar Alizadeh for suggestions on amine functionalization of silicon substrates, Prof. Jacob Israelachvili for the use of the UV/ozone cleaner, Jayna Jones and Dr. Uri Raviv for performing the SAXS measurement, and Dr. Tom Mates for assistance with the SIMS and XPS measurements. Portions of this research were carried out at the Stanford Synchrotron Radiation Laboratory, a national user facility operated by Stanford University on behalf of the U.S. Department of Energy, Office of Basic Energy Sciences. R.H. gratefully acknowledges support from the U.S. National Science Foundation for a Graduate Research Fellowship and the Corning Foundation for a Fellowship in Materials Research. This work was supported by the MRSEC Program of the National Science Foundation under Award DMR-00-80034. Additional support was provided through the National Science Foundation Division of Materials Research under award DMR-02-33728.

The importance of crosslinking the block-copolymer film to limit structural reorganization during templating in the approach demonstrated here can be seen directly from the field-emission scanning electron microscopy (FE-SEM) image in Figure 2. In this case, a polymer/silica hybrid material was formed from a dPS-*b*-P2VP film without first crosslinking the polymer film. The cylindrical structure of the block copolymer is retained, because the glassy nature of the dPS block (glass-

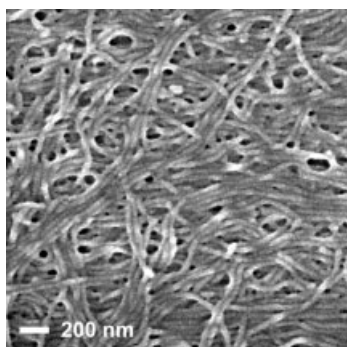


**Figure 2.** FE-SEM image of a hybrid silica/block-copolymer film produced by immersion of a non-crosslinked dPS-*b*-P2VP film in an aqueous silica precursor solution. The top portion of the film detached during swelling, providing a clear view of the internal morphology of the film.

transition temperature,  $T_g \sim 100^\circ\text{C}$  for bulk polystyrene) prevents reorganization into other, e.g., spherical morphologies. However, the initially well-ordered two-dimensional (2D) hexagonal morphology has been lost, replaced by a disordered collection of crisscrossing cylinders, indicating that significant rearrangement of individual cylinders has occurred during the swelling process.<sup>[18]</sup>

To prevent the mesostructured block-copolymer template species from rearranging extensively during swelling, the P2VP component was crosslinked by quaternization with 1,4-diiodobutane (DIB).<sup>[19]</sup> The block-copolymer films employed here were  $\sim 90$  nm thick and had 8–11 % of the P2VP moieties quaternized by DIB, as measured via X-ray photoelectron spectroscopy (XPS) (film thickness and the degree of crosslinking are both important variables in determining the morphologies of the resulting inorganic/block-copolymer films, as elucidated in a separate report).<sup>[20]</sup> Dynamic secondary-ion mass spectrometry (SIMS) was employed to measure the extent of crosslinking as a function of depth from the film surface. The iodine ( $^{127}\text{I}^-$ ) signal in the SIMS depth profile shown in Figure 3a is relatively constant, indicating homogeneous incorporation of the iodine-containing crosslinking agent.<sup>[21]</sup> The deuterium ( $^2\text{H}^-$ ) signal arising from the dPS component of the film oscillates as a function of depth, reflecting the organization of the block-copolymer structure

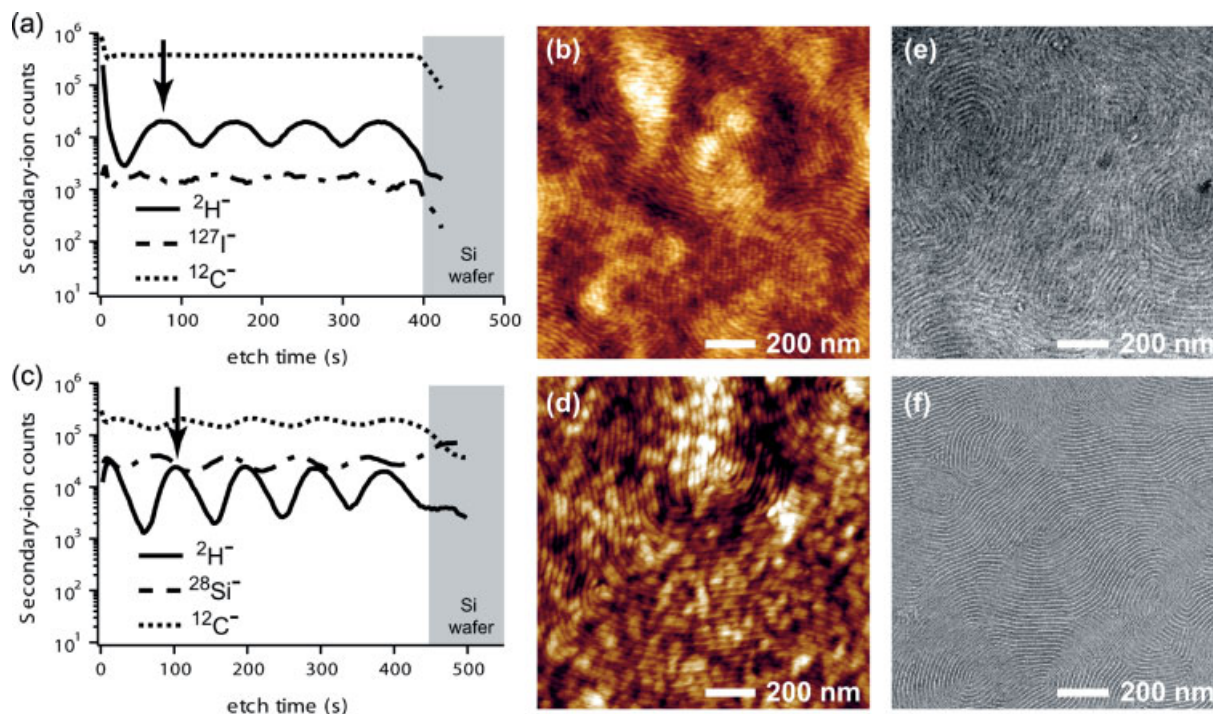


**Figure 3.** a) SIMS depth profiles of different elemental substituents ( $^2\text{H}^-$ ,  $^{127}\text{I}^-$ , and  $^{12}\text{C}^-$ ) in a crosslinked dPS-*b*-P2VP film consisting of four layers of dPS cylinders (100 nm thick following crosslinking). The arrow denotes the midpoint of the first layer of dPS cylinders, where a subsequent etch was halted for scanning force microscopy (SFM) imaging. b) SFM image of the same SIMS-etched crosslinked block-copolymer film. Brighter areas are higher than dark areas, with a total height scale of 3 nm. c) SIMS depth profiles ( $^2\text{H}^-$ ,  $^{28}\text{Si}^-$ , and  $^{12}\text{C}^-$ ) for a mesostructured crosslinked block-copolymer/silica film consisting of four layers of dPS cylinders (now 180 nm thick), and d) corresponding SFM image with a height scale of 10 nm. e) Transmission electron microscopy (TEM) image of a mesostructured crosslinked block-copolymer/silica film. f) TEM image of the mesoporous silica film formed after UV/ozone treatment of the crosslinked dPS-*b*-P2VP/silica hybrid film shown in (e).

with (10) planes of the 2D hexagonal structure parallel to the film plane. A peak in the deuterium signal at the free surface reveals a thin layer of dPS at the top of the film, while the four subsequent peaks indicate the presence of four layers of the dPS cylinders below. The deuterium signal is at a minimum value at the silicon substrate, reflecting preferential wetting of this interface by P2VP. Comparison of the film thickness measured by ellipsometry prior to crosslinking (90 nm) with the SIMS depth profile reveals that the layers of cylinders were spaced by  $20 \pm 0.5$  nm. This is in good agreement with a value of 20.5 nm, which was measured for the spacing between (10) planes in a bulk sample (see Supporting Information). The spacing between layers dilated slightly upon incorporation of the crosslinking agent; for the conditions employed here it increased by 5–10%. The in-plane morphology of the crosslinked block-copolymer film can be seen from the scanning force microscopy (SFM) image in Figure 3b. A series of stripes meander in the plane of the film giving rise to a “fingerprint” pattern that is characteristic of a 2D hexagonal structure with cylinders oriented parallel to the film plane.<sup>[22]</sup> The in-plane spacing between stripes is  $\sim 24$  nm, which corresponds closely to the inter-cylinder spacing in bulk dPS-*b*-P2VP samples (23.7 nm).

Silica was incorporated into a crosslinked dPS-*b*-P2VP template film by soaking for 12–15 h in an acidic aqueous silica precursor solution, as described in more detail in the Experimental section. During this time silica precursors diffused into the P2VP regions, where they were then condensed.<sup>[23–27]</sup> The incorporation of silica species into the film led to an increase in the dry film thickness,  $\sim 80\%$  over its initial value, and SIMS depth profiling (Fig. 3c) showed a strong  $^{28}\text{Si}^-$  signal throughout the film thickness. Oscillation of the  $^2\text{H}^-$  signal in the SIMS profile indicates that the out-of-plane ordering of the block-copolymer mesostructure was retained during silica infiltration. An oscillation of the  $^{12}\text{C}^-$  signal was apparent as well, because the silica-swelled P2VP block has a lower density of carbon atoms than the unswelled dPS. The silicon SIMS signal oscillates nearly out-of-phase with that of both deuterium and carbon, as expected for incorporation of a silica precursor into the P2VP domain of the polymer.<sup>[28]</sup> SFM and transmission electron microscopy (TEM) images of the silica/block-copolymer composite film in Figures 3d,e, respectively, reveal that the characteristic “fingerprint” morphology of the initial 2D hexagonal block-copolymer mesostructure has also been preserved. The presence of silicon in the P2VP component provides contrast between the polymer blocks in TEM (Fig. 3e), thus eliminating the need for staining. Notably, the composite mesostructure shows the same in-plane spacing between cylinders (24 nm) as the initial template, indicating that incorporation of silica has occurred by swelling of the block-copolymer structure normal to the film plane, without significant in-plane reorganization.

The block-copolymer template species were removed by UV/ozone treatment<sup>[29,30]</sup> or thermal oxidation to produce a mesoporous silica film. Ellipsometric measurements of such

mesoporous silica films in contact with air yielded refractive indices,  $n$ , in the range 1.36–1.39, which are significantly lower than that of bulk silica ( $n = 1.456$ ), reflecting the porous nature of the films. However, it is difficult to obtain an accurate measure of film porosities from these values due to adsorption of water from the atmosphere. The TEM image in Figure 3f shows that the resulting mesoporous silica film retains the same “fingerprint” morphology as the initial dPS-*b*-P2VP template and the hybrid composite. Further evidence for the preservation of in-plane ordering during incorporation of silica and UV/ozone treatment was obtained via cross-sectional TEM imaging of similar samples (see Supporting Information). While the mesostructural ordering in the films studied here is comparable to that in mesoporous films prepared by existing approaches,<sup>[1–4]</sup> an important distinction is that the structures prepared here are essentially replicas of the pre-organized block-copolymer templates. This approach, when coupled with strategies for manipulating domain orientation and long-range ordering in block-copolymer thin films,<sup>[13]</sup> may enable superior control of structure in mesoporous inorganic thin films.

An attractive feature of the technique presented here is that films of the same block-copolymer template can potentially be used to form a variety of different mesostructured and mesoporous inorganic materials with well-controlled morphologies. For example, mesoporous films with crystalline titania frameworks are of technological interest for applications such as solar cells<sup>[31]</sup> and photocatalysts.<sup>[32]</sup> As in the case of silica, previous approaches involving simultaneous assembly of amphiphilic structure-directing agents and inorganic sol-gel species have been successful for the preparation of semicrystalline titania films with well-controlled mesostructures.<sup>[33–37]</sup> The approach presented here can also be extended to the case of titania, which may provide a route to improved control of long-range ordering and orientation in thin films of mesoporous titania.

To prepare mesoporous titania films, an annealed and crosslinked dPS-*b*-P2VP block-copolymer film was immersed for 12–15 h in an aqueous solution of the water-soluble titania precursor titanium(IV) bis(ammonium lactato)dihydroxide (TALH). Titania species were effectively incorporated into the P2VP component of the block-copolymer film and subsequently condensed, leading to a significant increase in film thickness (typically  $\sim 80\%$ ). As shown in Figure 4a, SIMS depth profiling revealed that large amounts of titanium were present throughout the film thickness, and that the out-of-plane ordering of the block-copolymer mesostructure was retained in the hybrid film. A TEM image of a UV/ozone-treated mesoporous titania film is shown in Figure 4b, establishing also that the characteristic “fingerprint” in-plane morphology was preserved throughout processing of the film. Electron diffraction from the UV/ozone-treated titania film (Fig. 4b) indicates that the mesoporous titania film was at least partially crystalline. The radial spacings of the diffraction rings are consistent with anatase titania, which is the crystalline polymorph

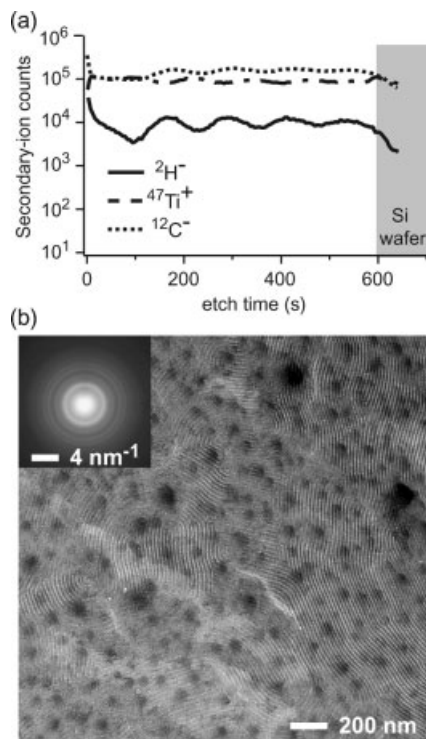


**Figure 4.** a) SIMS depth profiles ( $^2\text{H}^-$ ,  $^{47}\text{Ti}^+$ , and  $^{12}\text{C}^-$ ) for a mesostructured crosslinked block-copolymer/titania film consisting of four layers of dPS cylinders (180 nm thick following infiltration of titania precursors). b) TEM image of a mesoporous titania film (thickness  $\sim 80$  nm) prepared by UV/ozone treatment of the dPS-*b*-P2VP/titania film characterized by SIMS in (a). The dark spots correspond to  $\text{TiO}_2$  particles precipitated on the film surface during processing; these also contribute to a broadening of features in the SIMS depth profiles in (a). Inset: selected-area electron-diffraction pattern showing a series of diffraction rings indicating the presence of anatase  $\text{TiO}_2$  nanocrystals distributed homogeneously throughout the film.

typically formed from TALH at low temperatures.<sup>[38]</sup> The dark regions,  $\sim 40$ – $100$  nm, observed in Figure 4b appear from FE-SEM images to be particles of titania deposited on the film surface during infiltration of the precursor.<sup>[39,40]</sup> Dark-field TEM images (not shown here) revealed clearly that anatase nanocrystallites were homogeneously distributed throughout the film. Unlike the mesostructured and mesoporous silica films, microcracking of the titania films was frequently observed, most likely due to a large volume contraction upon conversion from TALH to titania. For applications where micro-cracking of the mesoporous titania film surface is undesirable further efforts are underway to optimize the robustness of the mesoporous titania network and its preparation.

In summary, crosslinking of the continuous P2VP component of a poly(*d*<sub>8</sub>-styrene)-*block*-poly(2-vinylpyridine) block-copolymer film is an effective way to limit mesostructural reorganization during swelling and infiltration of inorganic sol-gel precursor species. In this manner, mesoporous silica and titania films were formed with morphologies that were directly related to those of the pre-formed block-copolymer template films.

## Experimental

dPS-*b*-P2VP block copolymer was synthesized by standard anionic polymerization techniques [41]. Matrix-assisted laser desorption/ionization time-of-flight mass spectrometry indicated a molecular weight of  $33.3 \text{ kg mol}^{-1}$  with a polydispersity index (weight-average molecular weight/number-average molecular weight) of 1.01. The molar composition was determined to be 25% dPS from  $^{13}\text{C}$  solution-state NMR. Small-angle X-ray scattering indicated that, following annealing at  $210^\circ\text{C}$ , bulk samples formed a 2D hexagonal lattice of dPS cylinders with a lattice parameter  $a = 23.6$  nm (see Supporting Information).

Prior to film deposition, silicon substrates were cleaned by UV/ozone treatment and placed in a desiccator evacuated to 50 torr (1 torr  $\approx 133$  Pa) with 2 g of 3-aminopropyltriethoxysilane for at least 15 h to provide a surface coating of aminosilane. Amine functionalization was used to improve adhesion of the polymer films to the substrate and suppress osmotic-stress-induced film buckling [42]. The amine-functionalized silicon wafers were sonicated for 10 min in acetone and rinsed with ethanol to remove excess silane. Thin films of dPS-*b*-P2VP were prepared by spin-coating from a 2.5 wt.-% polymer solution in toluene, and film thicknesses were measured by null ellipsometry (Rudolph EL II). The films were subsequently annealed thermally under high vacuum ( $< 10^{-6}$  torr) at  $210^\circ\text{C}$ . Crosslinking of the P2VP component was accomplished by placing films into a desiccator evacuated to 50 torr with 100  $\mu\text{L}$  of 1,4-diiodobutane, and subsequently placed in a forced-convection oven at  $60 \pm 2^\circ\text{C}$  for 2.5–3.5 h. This crosslinking procedure rendered the polymer films insoluble in acidic water, methanol (selective solvents for P2VP), and tetrahydrofuran (a good solvent for both dPS and P2VP). All chemicals were obtained from Aldrich.

The degree of quaternization of the crosslinked block-copolymer films was measured via X-ray photoelectron spectroscopy (XPS) using a Kratos Axis Ultra XPS system with a monochromated aluminum X-ray source. The binding energy of the N1s electrons for pyridine units quaternized by DIB was 3.1 eV higher than that for unquaternized pyridine. The relative concentrations of each were determined by fitting Gaussian curves to the peaks for the two components.

Incorporation of silica was carried out by immersing the preformed dPS-*b*-P2VP films in an acidic (pH 0.0) solution containing 25 mM of pre-hydrolyzed silica precursor species for 12–15 h at  $20^\circ\text{C}$ , after which time the films were rinsed with deionized water. The silica precursor solution was formed by mixing 2.7 mL of 1.0 M HCl (aqueous) with 10  $\mu\text{L}$  of tetramethoxysilane for  $\sim 1$  min before immersion of the polymer films. Infiltration of titania was performed by immersing dPS-*b*-P2VP template films in an aqueous solution of 0.20 M TALH adjusted to pH 2.0 via addition of 1.0 M HCl for 12–15 h at  $20^\circ\text{C}$ . The polymer/titania films were subsequently removed from the precursor solution and washed with deionized water, then heated to  $80^\circ\text{C}$  under vacuum ( $\sim 10^{-2}$  torr) for 3 h to promote condensation of the titania precursor species. Block-copolymer/inorganic films were treated in a UV/ozone cleaner (UVOCS) for 1 h to oxidize and thereby remove the polymer template species to generate mesoporous inorganic structures. Alternatively, the block-copolymer species were removed by thermal oxidation in air by heating samples at  $1^\circ\text{C min}^{-1}$  to  $400^\circ\text{C}$  and holding at this temperature for 4 h.

Depth profiling of the different atomic components in the thin films was accomplished by SIMS using a Physical Electronics 6650 Dynamic SIMS system. A beam of  $\text{O}^{2+}$  ions accelerated through 2 kV was rastered across the film surface to form a 300  $\mu\text{m}$  crater. Negative secondary ions were collected, except for the case of titanium, where positive ions were collected. Films were prepared on a silicon wafer coated with 250 nm of silicon oxide to minimize drift of the signals due to charging effects. SFM was performed in SIMS craters where the film had been etched to the first sub-surface maximum in the  $^2\text{H}$ -signal, corresponding to the midpoint of the first layer of dPS cylinders. A Digital Instruments multimode Nanoscope IIIa SFM instrument was operated in tapping mode, and height-contrast images were collected. Differences in the speed with which the various components

of the film (i.e., dPS, P2VP, silica) are etched via SIMS gave rise to the height contrast observed in SFM [43].

FE-SEM images were collected with an FEI XL40 Sirion microscope using an accelerating voltage of 3 kV on samples coated with gold/palladium. TEM samples were prepared from films supported on silicon wafers by using a drop of 35 wt.-% aqueous poly(acrylic acid) (PAA) solution to remove the sample from the support and subsequently dissolving the PAA as the sample floated at an air/water interface. The TEM sample of the mesoporous silica film was produced by UV/ozone treatment of an existing TEM sample of a block-copolymer/silica hybrid film (UV/ozone treatment made it difficult to remove mesoporous silica films from the silicon substrates). Films were captured on a TEM grid and imaged using an FEI Tecnai G2 Sphera TEM operating at 200 kV.

Received: February 16, 2005

Final version: July 24, 2005

Published online: September 15, 2005

- [1] H. Yang, A. Kuperman, N. Coombs, S. Mamiche-Afara, G. A. Ozin, *Nature* **1996**, 379, 703.
- [2] Y. F. Lu, R. Ganguli, C. A. Drewien, M. T. Anderson, C. J. Brinker, W. L. Gong, Y. X. Guo, H. Soyez, B. Dunn, M. H. Huang, J. I. Zink, *Nature* **1997**, 389, 364.
- [3] D. Zhao, P. Yang, N. Melosh, J. Feng, B. F. Chmelka, G. D. Stucky, *Adv. Mater.* **1998**, 10, 1380.
- [4] G. J. de A. A. Soler-Illia, E. L. Crepaldi, D. Grosso, C. Sanchez, *Curr. Opin. Colloid Interface Sci.* **2003**, 8, 109.
- [5] D. Grosso, F. Cagnol, G. J. de A. A. Soler-Illia, E. L. Crepaldi, H. Amenitsch, A. Brunet-Bruneau, A. Bourgeois, C. Sanchez, *Adv. Funct. Mater.* **2004**, 14, 309.
- [6] H. W. Hillhouse, T. Okubo, J. W. van Egmond, M. Tsapatsis, *Chem. Mater.* **1997**, 9, 1505.
- [7] M. Trau, N. Yao, E. Kim, Y. Xia, G. M. Whitesides, I. A. Aksay, *Nature* **1997**, 390, 674.
- [8] H. Miyata, K. Kuroda, *Chem. Mater.* **1999**, 11, 1609.
- [9] H. Miyata, K. Kuroda, *J. Am. Chem. Soc.* **1999**, 121, 7618.
- [10] Y. Kawashima, M. Nakagawa, T. Seki, K. Ichimura, *Chem. Mater.* **2002**, 14, 2842.
- [11] V. R. Koganti, S. E. Rankin, *J. Phys. Chem. B* **2005**, 109, 3279.
- [12] Y. Yamauchi, M. Sawada, T. Noma, H. Ito, S. Furumi, Y. Sakka, K. Kuroda, *J. Mater. Chem.* **2005**, 15, 1137.
- [13] C. Park, J. Yoon, E. L. Thomas, *Polymer* **2003**, 44, 6725.
- [14] R. A. Pai, R. Humayun, M. T. Schulberg, A. Sengupta, J. N. Sun, J. J. Watkins, *Science* **2004**, 303, 507.
- [15] N. Nishiyama, S. Tanaka, Y. Egashira, Y. Oku, K. Ueyama, *Chem. Mater.* **2003**, 15, 1006.
- [16] S. Tanaka, N. Nishiyama, Y. Oku, Y. Egashira, K. Ueyama, *J. Am. Chem. Soc.* **2004**, 126, 4854.
- [17] G. S. Attard, J. C. Glyde, C. G. Göltner, *Nature* **1995**, 378, 366.
- [18] Adjacent cylinders in Figure 2 are spaced by 35–40 nm, which is considerably expanded from the value of 24 nm for the melt state, as seen in Figure 3b. The osmotic stresses generated during swelling of the thin polymer film were apparently alleviated by large-scale rearrangement of the initial 2D hexagonal mesostructure to allow cylinders to adopt an expanded nearest-neighbor spacing in-plane as well as out-of-plane.
- [19] R. Saito, S. Okamura, K. Ishizu, *Polymer* **1992**, 33, 1099.
- [20] R. C. Hayward, B. F. Chmelka, E. J. Kramer, *Macromolecules* **2005**, 38, 7768.
- [21] The iodine signal oscillates slightly due to the incorporation of DIB into the P2VP component of the polymer.
- [22] Virtually identical structures were observed for the block-copolymer film before and after P2VP crosslinking, indicating that the morphology is not significantly altered by the crosslinking procedure.
- [23] Details of the interaction between P2VP and silica are not yet well-understood. The mechanism is thought to involve enhanced condensation of silica in the presence of the block-copolymer template, and/or favorable interactions (i.e., hydrogen bonding) between P2VP moieties and the silica oligomers. There have been previous reports of silica templating by poly(vinylpyridine) under acidic conditions [24–26], and poly(2-vinylpyridine) is known to adsorb strongly on silica surfaces under highly acidic conditions [27].
- [24] E. Krämer, S. Förster, C. Göltner, M. Antonietti, *Langmuir* **1998**, 14, 2027.
- [25] G. Cho, J. Jang, S. Jung, I. S. Moon, J. S. Lee, Y. S. Cho, B. M. Fung, W. L. Yuan, E. A. O'Rear, *Langmuir* **2002**, 18, 3430.
- [26] N. Fujita, M. Asai, T. Yamashita, S. Shinkai, *J. Mater. Chem.* **2004**, 14, 2106.
- [27] J. Hahn, S. E. Webber, *Langmuir* **2004**, 20, 4211.
- [28] The silicon signal lags the deuterium signal by slightly more than half the period of the oscillation, presumably due to the slower etching of silica relative to polystyrene by the oxygen-ion beam of the SIMS instrument.
- [29] A. Hozumi, Y. Yokogawa, T. Kameyama, K. Hiraku, H. Sugimura, O. Takai, M. Okido, *Adv. Mater.* **2000**, 12, 985.
- [30] T. Clark, J. D. Ruiz, H. Fan, C. J. Brinker, B. I. Swanson, A. N. Parikh, *Chem. Mater.* **2000**, 12, 3879.
- [31] M. Grätzel, *Curr. Opin. Colloid Interface Sci.* **1999**, 4, 314.
- [32] N. Serpone, R. F. Khairutdinov, in *Semiconductor Nanoclusters—Physical, Chemical, and Catalytic Aspects* (Eds: P. V. Kamat, D. Meisel), Vol. 103, Elsevier, New York **1997**, p. 417.
- [33] D. Grosso, G. J. de A. A. Soler-Illia, F. Babonneau, C. Sanchez, P. A. Albouy, A. Brunet-Bruneau, A. R. Balkenende, *Adv. Mater.* **2001**, 13, 1085.
- [34] Y. K. Hwang, K. C. Lee, Y. U. Kwon, *Chem. Commun.* **2001**, 1738.
- [35] P. C. A. Alberius, K. L. Frindell, R. C. Hayward, E. J. Kramer, G. D. Stucky, B. F. Chmelka, *Chem. Mater.* **2002**, 14, 3284.
- [36] B. Smarsly, D. Grosso, T. Brezesinski, N. Pinna, C. Boissiere, M. Antonietti, C. Sanchez, *Chem. Mater.* **2004**, 16, 2948.
- [37] S. Y. Choi, M. Mamak, N. Coombs, N. Chopra, G. A. Ozin, *Adv. Funct. Mater.* **2004**, 14, 335.
- [38] A. Hanprasopwattana, T. Rieker, A. G. Sault, A. K. Datye, *Catal. Lett.* **1997**, 45, 165.
- [39] The particles were not deposited by sedimentation (films were immersed in the precursor solution in a vertical orientation) but apparently nucleated on the film surface. This most likely occurred due to the proximity of the processing conditions (pH and concentration) to the stability limits for the titania precursor, beyond which macroscopic precipitation of titania was observed [40].
- [40] S. Baskaran, L. Song, J. Liu, Y. L. Chen, G. L. Graff, *J. Am. Ceram. Soc.* **1998**, 81, 401.
- [41] H. Yokoyama, T. E. Mates, E. J. Kramer, *Macromolecules* **2000**, 33, 1888.
- [42] J. S. Sharp, R. A. L. Jones, *Phys. Rev. E* **2002**, 66, 011 801.
- [43] R. A. Segalman, H. Yokoyama, E. J. Kramer, *Adv. Mater.* **2001**, 13, 1152.